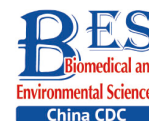


Original Article

**Phosphorylation of Cofilin-1 Enhances Paclitaxel Resistance of Epithelial Ovarian Cancer Cells by Inhibiting Apoptosis***

LI Min^{1,#}, DONG Xu Dong², LYU Qiu Bo¹, ZHANG Wei³, HUANG Shuai¹,
YANG Chun Xue⁴, CUI Di², and LAI Hui Ying⁵

1. Department of Obstetrics and Gynecology, Beijing Hospital, National Center of Gerontology, Institute of Geriatric Medicine, Chinese Academy of Medical Sciences, Beijing 100730, China; 2. Department of Obstetrics, the First People's Hospital of Yunnan Province, Kunming 650032, Yunnan, China; 3. Department of Pathology, Beijing Hospital, National Center of Gerontology, Institute of Geriatric Medicine, Chinese Academy of Medical Sciences, Beijing 100730, China; 4. Peking University Health Science Center, Beijing 100069, China; 5. Clinical Laboratory, Beijing Hospital, National Center of Gerontology, Institute of Geriatric Medicine, Chinese Academy of Medical Sciences, Beijing 100730, China

Abstract

Objective To investigate the molecular mechanism of high phosphorylation levels of cofilin-1 (p-CFL-1) associated with paclitaxel resistance in epithelial ovarian cancer (EOC) cells.

Methods Cells displaying varying levels of p-CFL-1 and CFL-1 were created by plasmid transfection and shRNA interference. Cell inhibition rate indicating paclitaxel efficacy was assessed by Cell Counting Kit-8 (CCK-8) assay. Apoptosis was assessed by flow cytometry and protein levels were detected by western blotting. Quantitative real-time polymerase chain reaction (qRT-PCR) was used to measure the expression levels of phosphokinases and phosphatases of CFL-1. Survival analysis evaluated the correlation between the prognosis of EOC patients and the levels of p-CFL-1 and slingshot-1 (SSH-1).

Results High levels of p-CFL-1 were observed in EOC cells that survived treatment with high doses of paclitaxel. SKOV3 cell mutants with upregulated p-CFL-1 showed impaired paclitaxel efficacy, as well as decreased apoptosis rates and pro-survival patterns of apoptosis-specific protein expression. Cytoplasmic accumulation of p-CFL-1 inhibited paclitaxel-induced mitochondrial apoptosis. SSH-1 silencing mediated CFL-1 phosphorylation in paclitaxel-resistant SKOV3 cells. Clinically, the high level of p-CFL-1 and the low level of SSH-1 in EOC tissues were closely related to chemotherapy resistance and poor prognosis in EOC patients.

Conclusion The SSH-1/p-CFL-1 signaling pathway mediates paclitaxel resistance by apoptosis inhibition in EOC and is expected to be a potential prognostic predictor.

Key words: Cofilin-1; Slingshot-1; Epithelial ovarian cancer; Chemo-resistance; Apoptosis

Biomed Environ Sci, 2021; 34(6): 465-477 doi: 10.3967/bes2021.063

ISSN: 0895-3988

www.besjournal.com (full text)

CN: 11-2816/Q

Copyright ©2021 by China CDC

*National Natural Science Foundation of China [No. 81302277]; Beijing Dongcheng District Excellent Talents Funding Project [No. 2018-13]; Yunnan Provincial Department of Science and Technology – 2020 Kunming Medical University Joint Special Project on Applied Basic Research [No. 202001AY070001-128].

#Correspondence should be addressed to LI Min, MD Tel: 86-13811526308 Fax: 86-10-85136220 E-mail: limin3744@bjhmoh.cn

Biographical note of the first author: LI Min, female, born in 1973, Doctor of Medicine, Chief Physician, majoring in gynecological oncology and pelvic floor disorders.

INTRODUCTION

Epithelial ovarian cancer (EOC) is the leading cause of death among gynecological malignancies globally, with an overall 5-year survival rate of only 26% to 46%^[1]. Much progress has been made in the treatment of ovarian cancer in the past few decades^[2-4]. The standard treatment strategy of EOC is cytoreductive surgery followed by cisplatin and paclitaxel-based chemotherapy^[1,5]. Although more than 80% of patients initially respond well to standard treatment, chemotherapy resistance remains a critical therapeutic obstacle and one of the most common causes of death^[5,6]. Elucidating the specific molecular mechanism of chemotherapy resistance and exploring the key factors to reverse drug resistance have important clinical significance for improving the survival rate of ovarian cancer patients.

In previous studies, we found that phosphorylated cofilin-1 (p-CFL-1) was overexpressed in paclitaxel-resistant EOC cell lines (SK-TR30, SK-TR2500, and A2780-TR) and ovarian cancer tissues by two-dimensional gel electrophoresis, matrix-assisted laser desorption ionization-time-of-flight-mass spectrometry (MALDI-TOF-MS), and immunohistochemistry (IHC) assays^[7]. Cofilin-1 (CFL-1), a member of the actin-binding protein family, plays an essential role in the regulation of actin filament dynamics^[8,9]. Serine-3 (Ser-3) is the only phosphorylation site in CFL-1. Through phosphorylation and dephosphorylation of Ser-3, the activity of CFL-1 is specifically regulated by protein kinases such as LIM-kinases (LIMKs) and testicular protein kinases (TESKs), as well as phosphatases such as slingshot (SSH) family members and chronophin^[8,9]. The regulation of CFL-1 phosphorylation is a key link between extracellular stimulation and actin cytoskeleton dynamics. Abnormally phosphorylated CFL-1 activity plays an important role in many pathological conditions, such as neurological and cardiovascular diseases, tumor metastasis and invasion, and drug resistance^[9-16]. Our group focuses on EOC chemo-resistance and is among the first groups to report p-CFL-1 as a trigger for chemotherapy resistance^[7,9,15,16]. However, the exact mechanism of drug resistance in EOC cells related to CFL-1 phosphorylation is still unclear. This study aimed to reveal the impact of p-CFL-1 on paclitaxel resistance in EOC cells. We confirmed that SSH-1 regulated the phosphorylation of CFL-1 at Ser-3 to prevent SKOV3 cells from paclitaxel resistance resulting from apoptosis inhibition. We also observed that the levels

of SSH-1/CFL-1 were closely related to the response of EOC patients to paclitaxel and their prognosis.

MATERIALS AND METHODS

Cell Culture

The SKOV3 cell line was kindly provided by Prof. YANG (State Key Laboratory of Biotherapy and Cancer Center/Collaborative Innovation Center for Biotherapy, West China Hospital, Sichuan University, Chengdu, China). The SK-TR30 cell line is a stable paclitaxel-resistant cell line^[7]. The human ovarian cancer cell lines A2780 and A2780-TR were kindly provided by Dr. LI (Department of Obstetrics and Gynecology, Guangxi Cancer Hospital, Guangxi Medical University, Nanning, China). SKOV3 and SK-TR30 cells were grown in high glucose DMEM (DMEM/HG) medium supplemented with 10% fetal bovine serum. A2780 and A2780TR cells were grown in RPMI-1640 medium supplemented with 10% fetal bovine serum. These cells were grown at 37 °C in a humidified atmosphere containing 5% CO₂. SK-TR30 and A2780-TR cells were cultured in medium containing an additional 10 nmol/L paclitaxel to maintain drug resistance and further cultured in drug-free medium for one week before follow-up experiments. Once thawed, the cell lines were routinely authenticated approximately every 6 months.

Reagents and Antibodies

Antibodies against CFL-1 (#ab42824), p-CFL-1 (#ab12866), SSH-1 (#ab76943), Bcl-2 (#ab59348), caspase-3 (#ab13847), Cytochrome c (#ab90529), and GAPDH (#ab70699) were purchased from Abcam (USA). HRP-conjugated anti-mouse and anti-rabbit antibodies (#7076 and #7047, respectively) were obtained from Cell Signaling Technology (USA). Anti-SSH-1 antibody used in the immunohistochemistry (IHC) assay was supplied by ECM Biosciences LLC (#SP1711, Kentucky, USA). Paclitaxel was purchased from Cell Signaling Technology (#98075).

Plasmid Constructs and Transfection

Plasmids with ectopic overexpression of CFL-1 or p-CFL-1 [including WT (wild type), S3A (phosphodeficient cofilin mutant, Ser-3 replaced with alanine) and S3D (phosphomimetic cofilin mutant, Ser-3 replaced with an aspartate)], overexpression of human SSH-1 and non-targeting negative-control targets were supplied by Vigene Bioscience (Shandong, China). CFL-1 and SSH-1 shRNAs were also purchased from Vigene Bioscience. Plasmids were transfected in ovarian

cancer cells using Lipo3000-based Transfection Reagent (System Invitrogen Inc., Palo Alto, CA, USA), according to the manufacturer's instructions.

Western Blotting

Whole-cell and cytoplasmic proteins were extracted using a ProteoJET Kit (Fermentas, USA). Mitochondrial proteins were isolated using a ReditPrep™ Mitochondrial/Cytoplasmic Fractionation Kit (AAT Bioquest, USA). Equal amounts of proteins were separated by SDS-PAGE and transferred onto polyvinylidene fluoride membranes (Millipore, Bedford, MA, USA). The membranes were incubated with primary antibodies at 4 °C overnight, then probed with the appropriate secondary antibodies for 1 h at room temperature. GAPDH was used as the endogenous control. The bands were visualized and quantitated using the ECL Advance Detection System (Millipore, Billerica, MA, USA).

Quantitative Real-time PCR (qRT-PCR) Assay

Total RNA was extracted using TRIzol Reagent (TAKARA, Japan) according to the manufacturer's instructions. First-strand cDNA was generated using the PrimeScript RT reagent Kit (TAKARA). qPCR was performed using SYBR Premix Ex Taq Kits (Takara, Dalian, China) according to the manufacturer's introductions. For real-time PCR analysis, the following primers were used: *LIMK-1* forward, 5'-AGATGAGGCTGGGATGGACA-3', reverse, 5'-GTGG-AGCACTCCAAGCTGTA-3'; *LIMK-2* forward, 5'-AAGCTCTACTGCCCAAGGA-3', reverse, 5'-ATATGCATCCCCATCTCAA-3'; *SSH-1* forward, 5'-AGTCTTCAGCACCCCCACAA-3', reverse, 5'-GTCTTCGCAACGCAGAAGGT-3'; *SSH-2* forward, 5'-TCTCTGGAGCGACACGCTAA-3', reverse, 5'-CACATTGCCTGCACAGATACA-3'; *SSH-3* forward, 5'-CTTGCCCTCTGGAGTGACA-3', reverse, 5'-TGGATGGAGATGGGCTTGAA-3'; *TESK-1* forward, 5'-GGCCGAAAAGATTCCTGTGT-3', reverse, 5'-CAGCTACCCCCGTAACACCT-3'; and *TESK-2* forward, 5'-GCATTTGCCTTGGACTGTGA-3', reverse, 5'-CTTCTCAGCCAGGCCAAAGT-3'. The reference gene β -actin was used as the internal control for RNA quality. The $2^{-\Delta\Delta Ct}$ method was used to evaluate the gene expression fold change among the groups. All experiments were performed in triplicate.

Cytotoxicity Assay

SKOV3 cells were transfected with plasmids and shRNA for 24 h. Then, cells were seeded into 96-well plates at a density of 4×10^3 cells/well. SKOV3 cells were exposed to paclitaxel at various concentrations (0, 2, 10, 20, 50, 100, and 200 nmol/L) for another 72 h

after adhering to the plates. The Cell Counting Kit-8 (CCK-8) solution was added into each well at 0, 24, 48, and 72 h, and the cells were incubated in a 5% CO₂ incubator at 37 °C for 2 h. Finally, the OD value was measured at 450 nm using a microplate reader (Bio-Tek, Winooski, VT, USA) and surviving fractions were calculated. Cell survival was calculated by normalizing the absorbance of untreated controls. The half-maximal inhibitory concentration (IC₅₀) was used to reflect cell viability following paclitaxel treatment. The IC₅₀ was obtained from the dose-response curves using Graph-Pad Prism 5.0 program (GraphPad Software, Inc.).

Wound-healing and Transwell Invasion Assay

At 48 h after transfection with WT, S3D, S3A, shCFL1, and control vectors, 5×10^5 cells/well were seeded into six-well plates. The cells were scraped with a 200 μ L pipette tip when they achieved 90% confluency. After washing with phosphate-buffered saline, the scraped cells were then cultured for another 24 h. Images were captured at 0 and 24 h under a light microscope. All experiments were performed in triplicate.

Cellular invasion assay was performed using Matrigel Invasion Chambers (BD Biosciences) with inserts containing an 8 μ m pore-sized membrane with a thin layer of Matrigel. Cells were seeded into the upper chamber of 24-well Transwell plates at a density of 5×10^4 cells/well with serum-free medium after transfection. The bottom chamber was filled with 500 μ L completed medium containing 10% fetal bovine serum. The Transwell-containing plates were incubated for 8 h. The upper chamber was washed, fixed with 70% ethanol, and stained with 0.1% crystal violet (Solarbio, C8470) for 20 min at room temperature. The cells remaining on the upper surface of the filter membrane were removed with a cotton swab. The invasive cells on the bottom of the membrane were stained and three different fields of stained cells were counted under a light microscope.

Apoptosis Assay

Prior to exposure to 10 nmol/L paclitaxel, all cells in exponential growth phase were transfected with overexpression and knockdown plasmids for 48 h. The degree of apoptosis was measured using an Annexin V Apoptosis Detection Kit (BD Biosciences, San Diego, CA, USA), according to the manufacturer's protocol. The harvested cell suspension was incubated with annexin V for 15 min at room temperature in the dark and then detected by FACSCalibur flow cytometry (BD Biosciences). The cell

apoptosis rate was analyzed using CellQuest software (BD Biosciences).

Patient-specimen Selection and Immunohistochemistry Assay

For IHC analysis, we obtained formalin-fixed and paraffin-embedded tissue samples from 108 patients with FIGO stage I–IV EOC. All EOC patients involved underwent primary cytoreduction and subsequent paclitaxel-based chemotherapy in our hospital between February 2013 and June 2016. The date of the latest record retrieved was June 30, 2019. The clinical characteristics, pathologic diagnoses, and outcome information were collected from the patients' medical records and pathologic slides. The clinical and pathological features are shown in Table 1. Overall survival time (OS) was calculated as the time from surgery to the last follow-up date or death. Progression-free survival time (PFS) was calculated as the time from surgery to the time of detected recurrence or progression. Both OS and PFS were calculated from the date of pathologic diagnosis. EOC patients with PFS \leq or $>$ 6 months were divided into "sensitive" and "resistant" to paclitaxel-based chemotherapy groups, respectively. This study has been approved by the Beijing Hospital Medical Ethics Committee (BJ-2019BJYEC-029-01) and registered at www.chictr.org.cn. Analysis of IHC was performed as previously described^[7], with anti-p-CFL-1 (1:300) and anti-SSH-1 (1:100) antibodies. All staining was performed with HRP-conjugated anti-mouse or anti-rabbit IgG secondary antibody and visualized

by DAB. Dr. Z. W. confirmed all of the pathological diagnoses, and was blinded to the clinical parameters. Staining was scored using a Foutier scale according to the percentage of positive cells and staining intensity: (–) or 0, tissue specimens without staining (0%–10%); (+) or 1, tissue specimens with weak staining (10%–25%); (++) or 2, tissue specimens with moderate staining (25%–50%) and (+++) or 3, tissue specimens with strong staining ($>$ 50%). (–) and (+) were defined as low expression, and (++) and (+++) were defined as high expression (or overexpression)^[7].

Statistical Analysis

Statistical analysis was performed with SPSS 22.0 and GraphPad Prism 5.0 software. The data were expressed as mean \pm SD/SEM ($M \pm s/sx$). Student's *t*-test and one or two-way ANOVA were used as appropriate for experiment and treatment groups. The correlation between p-CFL-1 and SSH-1 expression in EOC patient tissues was analyzed by Spearman's χ^2 test. Survival curves were generated according to the Kaplan–Meier method, and statistical analysis was performed using the log-rank test. A *P*-value of less than 0.05 was regarded as statistically significant.

Ethics Approval and Consent to Participate

This study was approved by the Ethics Committee of Beijing Hospital (2019BJYEC-029-01) and was registered at www.chictr.org.cn (ChiCTR1900021718). Written informed consent was obtained from all participants.

Table 1. Correlation between the clinicopathological features of EOC patients and the expression of SSH-1 or p-CFL-1

Clinicopathologic features	Relative p-CFL-1 level		χ^2 value	<i>P</i> value	Relative SSH-1 level		χ^2 value	<i>P</i> value
	Low, <i>n</i> (%)	High, <i>n</i> (%)			Low, <i>n</i> (%)	High <i>n</i> (%)		
Age (y)								
< 60	26 (60.47)	17 (39.53)	1.694	0.193	23 (53.49)	20 (46.51)	0.038	0.846
\geq 60	31 (47.69)	34 (43.31)			36 (55.38)	29 (44.62)		
FIGO staging								
I–II	20 (57.14)	15 (42.86)	0.396	0.529	17 (48.57)	18 (51.43)	0.767	0.381
III–IV	37 (50.68)	36 (49.32)			42 (57.53)	31 (42.46)		
Differentiation								
G1-2	28 (70.00)	12 (30.00)	7.605	0.020*	21 (42.50)	29 (57.50)	5.992	0.014*
G3	29 (42.65)	39 (57.35)			38 (61.76)	20 (38.24)		
Chemotherapy response								
Sensitive	45 (61.64)	28 (38.36)	7.105	0.008**	34 (46.58)	39 (53.42)	5.896	0.015*
Resistant	12 (34.29)	23 (65.71)			25 (71.43)	10 (28.57)		

Note. * *P* < 0.05, ** *P* < 0.01.

RESULTS

Elevated p-CFL-1 in Response to Paclitaxel-protected EOC Cells Against Paclitaxel

With increased paclitaxel concentration, the levels of p-CFL-1 in A2780 and SKOV3 cells increased accordingly. However, there was no significant change in the content of total CFL-1 protein (Figure 1A). To further determine the relationship between p-CFL levels and paclitaxel treatment response, we transfected plasmids that could modify the phosphorylation state of CFL-1 into SKOV3 cells. Compared with cells transfected with the control vector, the cells overexpressing wild type CFL (WT) and p-CFL-1 (S3D) were more resistant to paclitaxel, as demonstrated by a lower cell inhibition rate [(IC₅₀, (1.709 ± 0.086) vs. (1.068 ± 0.110) μmol/L, *P* = 0.003, (2.077 ± 0.189) vs. (1.068 ± 0.110) μmol/L, *P* = 0.002)]. By contrast, the mutant S3A with downregulated p-CFL-1 production showed higher sensitivity to drug exposure [(IC₅₀, (0.607 ± 0.148) vs. (1.068 ± 0.110) μmol/L, *P* = 0.001)]. (Figure 1B, 1D-1). Similarly, when CFL-1 expression was knocked down by shRNA technology, SKOV3 cells were more sensitive to paclitaxel [(IC₅₀, (0.484 ± 0.327) vs. (0.962 ± 0.094) μmol/L, *P* = 0.005)] (Figure 1C, 1D-2). Collectively, these results indicated that elevated p-CFL-1 levels are implicated in a compromised paclitaxel response.

Cytoplasmic Accumulation of p-CFL-1 Inhibited Paclitaxel-induced Mitochondrial Apoptosis

We observed a remarkable difference in apoptosis rates between paclitaxel-resistant (SK-TR30 and A2780-TR) and paclitaxel-sensitive (SKOV3 and A2780) cell lines as assessed by flow cytometry with annexin V/propidium iodide (PI) double staining. Following treatment with 10 nmol/L paclitaxel for 24 h, the rates of apoptosis of paclitaxel-resistant cell lines were significantly lower than those of the corresponding sensitive cell lines [SK-TR30 vs. SKOV3, (4.11% ± 0.78%) vs. (12.07% ± 1.47%), *P* = 0.01; A2780-TR vs. A2780, (5.84% ± 1.23%) vs. (14.60% ± 2.50%), *P* = 0.01] (Figure 2A). These data suggest a putative role of apoptosis inhibition in the mechanism of paclitaxel resistance. To verify our hypothesis that phosphorylated CFL-1 inhibits apoptosis, we detected the apoptosis rate, as well as the expression of apoptosis-specific proteins in the aforementioned mutants that displayed different levels of p-CFL-1. The S3D mutant with upregulated phosphorylated CFL-1

demonstrated a significantly lower apoptosis rate than the S3A mutant that expressed dephosphorylated CFL-1 [S3D vs. S3A, (4.35% ± 0.58%) vs. (17.9% ± 2.36%), *P* < 0.01, Figure 2B, 2C]. The expression of apoptosis-specific proteins further confirmed the apoptotic effect of p-CFL-1 on SKOV3 cells, including anti-apoptotic regulator (Bcl-2) and apoptosis biomarkers (cytochrome c and caspase-3). Western blotting showed that expression of Bcl-2 was upregulated and expression of cytochrome c and caspase-3 was downregulated in the S3D mutant group compared with the control group (Figure 2D). Conversely, the S3A mutant and CFL-1 knockdown groups demonstrated downregulated Bcl-2 and upregulated cytochrome c and caspase-3 levels compared with the control group (Figure 2D).

Previous studies have shown that mitochondrial translocation of dephosphorylated CFL, the only form able to enter the mitochondria, induces apoptosis^[17-20]. To further elucidate how different phosphorylation states of cofilin and their respective distribution contribute to the paclitaxel response, we compared the cellular distribution of p-CFL-1 and total CFL-1 in paclitaxel-resistant and -sensitive EOC cell lines. Although there was no significant difference in cytoplasmic CFL-1 expression between paclitaxel-resistant and -sensitive cells, a significant decrease in mitochondrial CFL-1 expression was detected in SK-TR30 and A2780-TR cells, consistent with previous studies (Figure 2E-1, 2E-2). Expression of p-CFL-1 in paclitaxel-resistant cell lines mainly localized to the cytoplasm compared with paclitaxel-sensitive cell lines. Expression of p-CFL-1 was not detected in the mitochondria of all experimental groups (Figure 2E-1, 2E-3). Therefore, we speculated that p-CFL is prevented from mitochondrial translocation to further induce apoptosis, and thus accumulates in the cytoplasm, enabling the cell to survive paclitaxel treatment.

SSH-1 Silencing Mediated CFL-1 Phosphorylation in Paclitaxel-resistant SKOV3 Cells

We detected gene expression of four CFL phosphokinases (*LIMK-1*, *LIMK-2*, *TESK-1*, and *TESK-2*) and three CFL phosphatases (*SSH-1*, *SSH-2*, and *SSH-3*) in SK-TR30 and SKOV3 cells. Expression of *SSH-1* and *SSH-3* was downregulated, while expression of *TESK-2* and *LIMK-2* was upregulated in SK-TR30 cells (Figure 3A). *SSH-1* was selected for further study as it exhibited the largest difference in gene expression between paclitaxel-resistant and -sensitive cells.

The expression of *SSH-1* in SK-TR30 and A2780-

TR cells was substantially lower than that in SKOV3 and A2780 cells, and decreased gradually with increasing paclitaxel concentration (Figure 3B, 3C). In addition, there was a negative correlation between the level of SSH-1 and the level of p-CFL-1 (Figure 3D). We also found that overexpression of SSH-1

enhanced the killing effect of paclitaxel on SKOV3 cells, while knocking down SSH-1 had a protective effect against paclitaxel, contrary to the effect of p-CFL-1 as shown by the cytotoxicity assay (Figure 3E). Altogether, these data demonstrated that paclitaxel could trigger changes in SSH-1/p-CFL-1 signaling,

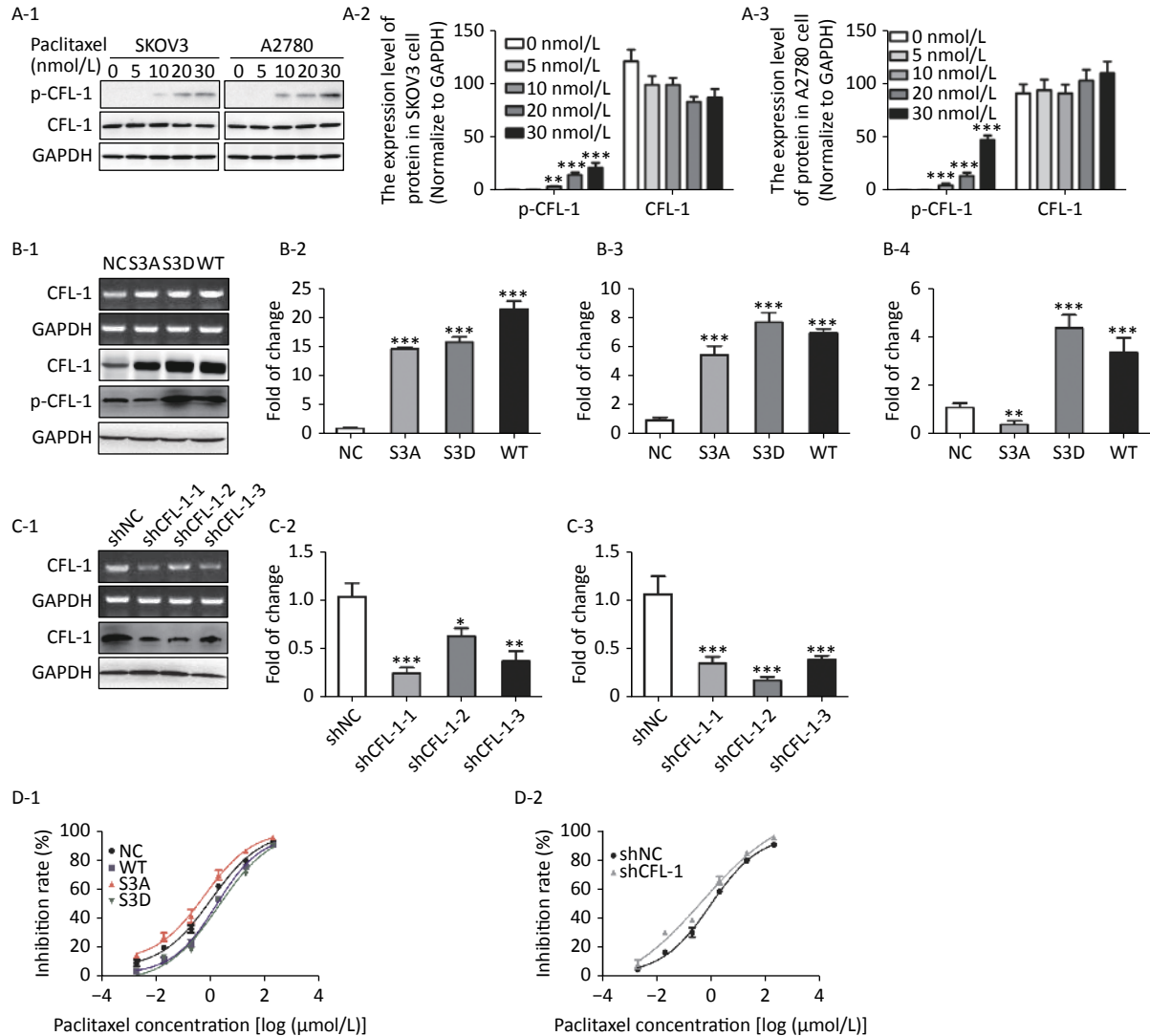


Figure 1. Effects of p-CFL-1 on paclitaxel resistance of EOC cells. (A-1 to A-3) Expression of p-CFL-1 and CFL-1 protein in EOC cells following treatment with different concentrations of paclitaxel. SKOV3 and A2780 cells were treated with 0, 5, 10, 20, and 30 nmol/L paclitaxel for 12 h. (B-1 to B-3) Gene and protein expression of CFL-1 increased in SKOV3 cells following transfection with S3A, S3D, and WT plasmids. (B-4) Protein expression of p-CFL-1 following transfection with S3A, S3D, and WT plasmids. (C-1 to C-3) Gene and protein expression of CFL-1 after CFL-1 knockdown by shRNA technology. (D-1) Inhibition rates following paclitaxel treatment of SKOV3 cells with different levels of p-CFL-1 after transfection with S3A, S3D, and WT plasmids. (D-2) Inhibition rates following paclitaxel treatment of SKOV3 cells with CFL-1 knockdown by shRNA. Three plasmids with overexpression of CFL-1: WT (wild type), S3A (phosphodeficient cofilin-1 mutant, Ser-3 replaced with alanine), and S3D (phosphomimetic cofilin-1 mutant, Ser-3 replaced with aspartate). Data are shown as means \pm SD of three independent experiments. * $P < 0.05$; ** $P < 0.01$, *** $P < 0.001$.

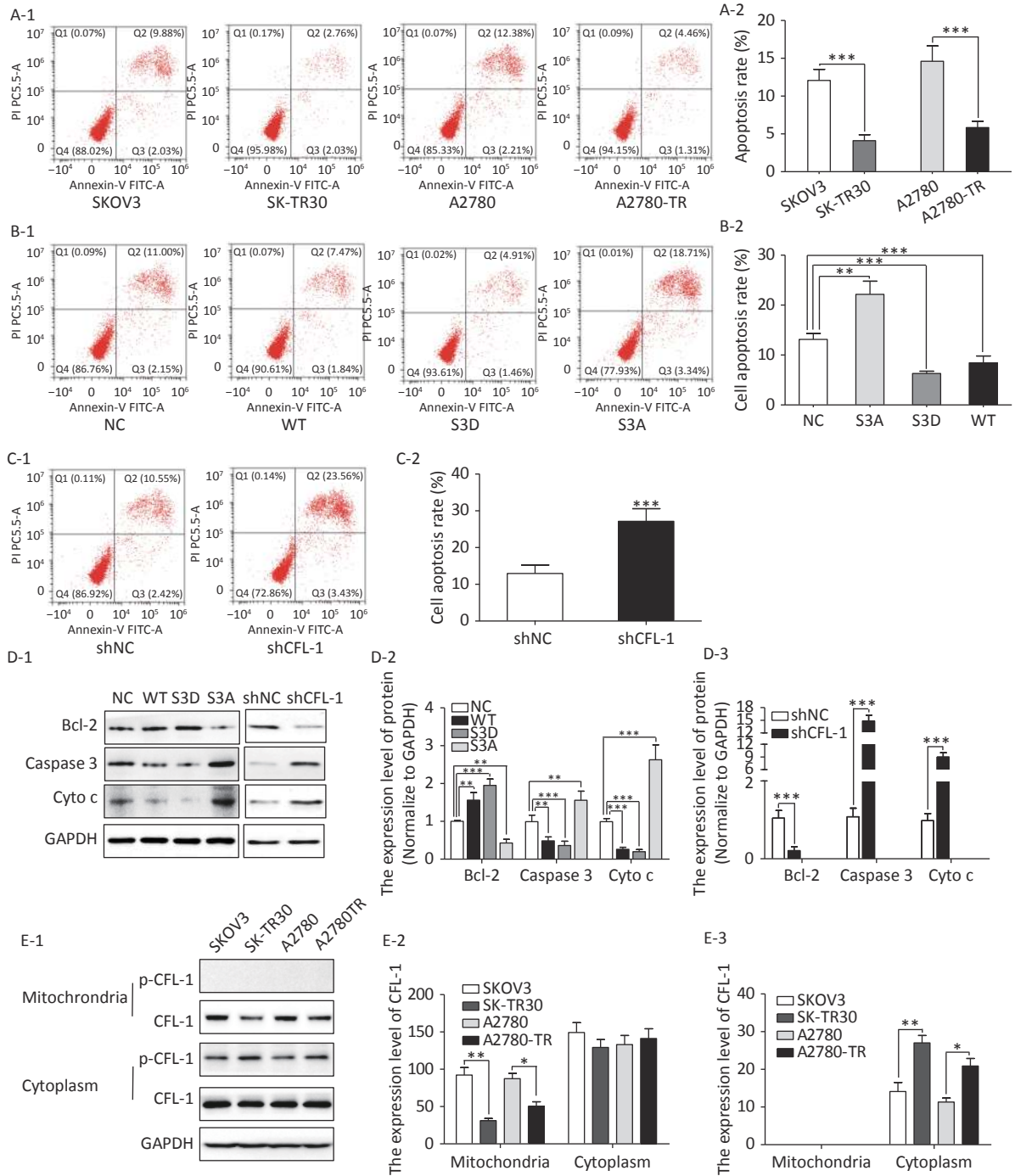


Figure 2. Phosphorylated-CFL-1 in the cytoplasm was associated with mitochondrial apoptosis under paclitaxel treatment. (A–C) Flow cytometry analysis of apoptosis by Annexin V and PI staining following treatment with 10 nmol/L paclitaxel. (A-1, A-2) Apoptosis rate of paclitaxel-sensitive (SKOV3 and A2780) and -resistant cells (SK-TR30 and A2780-TR). (B-1, B-2) Apoptosis rate of SKOV3 cells following transfection with S3A, S3D, and WT plasmids. (C-1, C-2) Apoptosis rate of SKOV3 cells after CFL-1 knockdown. (D-1 to D-3) Expression of Bcl-2, cytochrome c, and caspase-3 of SKOV3 cells following transfection with S3A, S3D, and WT plasmids, and of cells with CFL-1 knockdown. (E-1 to E-3) Cellular distribution of CFL-1 and p-CFL-1 protein expression in SKOV3 cells with different levels of p-CFL-1 and CFL-1. Error bars represent \pm SD; * $P < 0.05$; ** $P < 0.01$, *** $P < 0.001$.

which made EOC cells prone to paclitaxel resistance.

Low Expression of SSH-1 and High Expression of p-CFL-1 in EOC Tissues is Closely Correlated with chemo-resistance and Poor Prognosis of EOC Patients

To determine the clinical relevance of SSH-1/p-CFL-1 signaling, we investigated 108 EOC

patients, including 73 patients with chemo-resistance and 35 patients with chemo-sensitivity, all of whom underwent radical surgery followed by paclitaxel-based chemotherapy. The levels of p-CFL-1 and SSH-1 protein were analyzed by immunohistochemistry staining of tissue samples. The clinical characteristics of patients and the results of IHC analysis are shown in Table 1. High expression

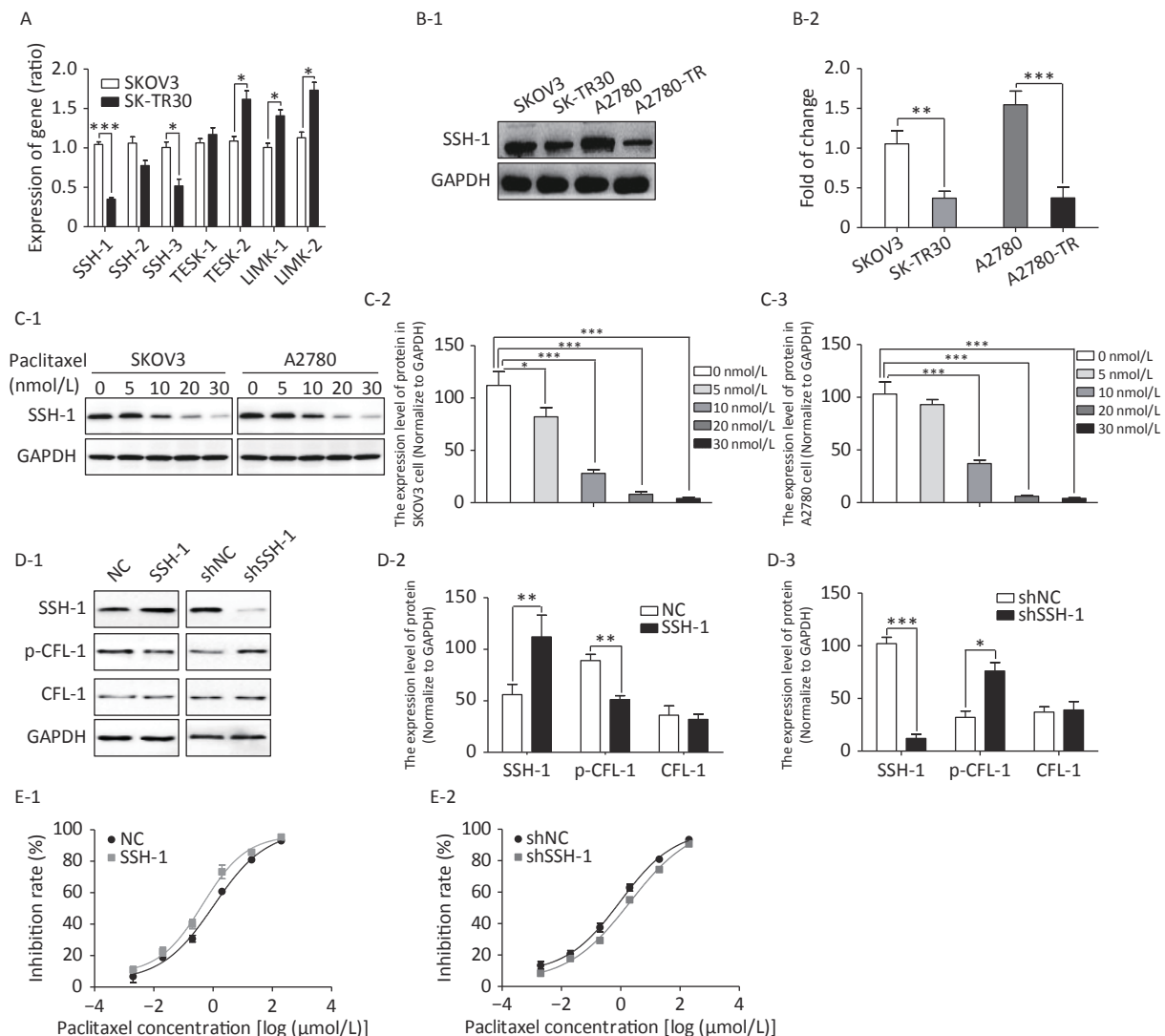


Figure 3. SSH-1 was responsible for upregulating p-CFL-1 to protect SKOV3 cells against paclitaxel. (A) Gene expression of CFL-1 phosphokinases and phosphatases as determined by qRT-PCR in SK-TR30 cells. (B-1, B-2) Expression of SSH-1 protein in paclitaxel-sensitive (SKOV3 and A2780) and -resistant (SK-TR30 and A2780-TR) EOC cells. (C-1 to C-3) Expression of SSH-1 protein in SKOV3 and A2780 cells following paclitaxel treatment. SKOV3 and A2780 cells were treated with 0, 5, 10, 20, and 30 nmol/L paclitaxel for 12 h. (D-1 to D-3) Expression of SSH-1 was negatively correlated with the expression of p-CFL-1. (E-1, E-2) Inhibition rates of SKOV3 cells under paclitaxel treatment with different levels of SSH-1 following transfection with SSH-1 plasmids and SSH-1 knockdown. The inhibition rate was calculated by determining the IC50 in every CCK-8 assay. The data are from at least three independent experiments. Error bars represent \pm SD; * $P < 0.05$; ** $P < 0.01$, *** $P < 0.001$.

of p-CFL-1 was negatively correlated with the differentiation of ovarian cancer, while expression of SSH-1 was positively correlated with the differentiation of EOC. As shown by immunohistochemistry staining, 65.71% (23/35) of chemo-resistant patients had high levels of p-CFL-1, and 71.43% (25/35) of chemo-resistant patients had low expression of SSH-1 (Figure 4A-1, 4B-1; Table 1).

Only 38.36% (28/73) of the patients had high expression of p-CFL-1, and 46.58% (34/73) of the patients had low expression of SSH-1 in the chemo-sensitive group, which was vastly different from that in the paclitaxel-resistant group. The coexistence of a low SSH-1 level and a high p-CFL-1 level accounted for 24.66% (13/73) of chemo-sensitive patients and 60.00% (21/35) of chemo-resistant patients with

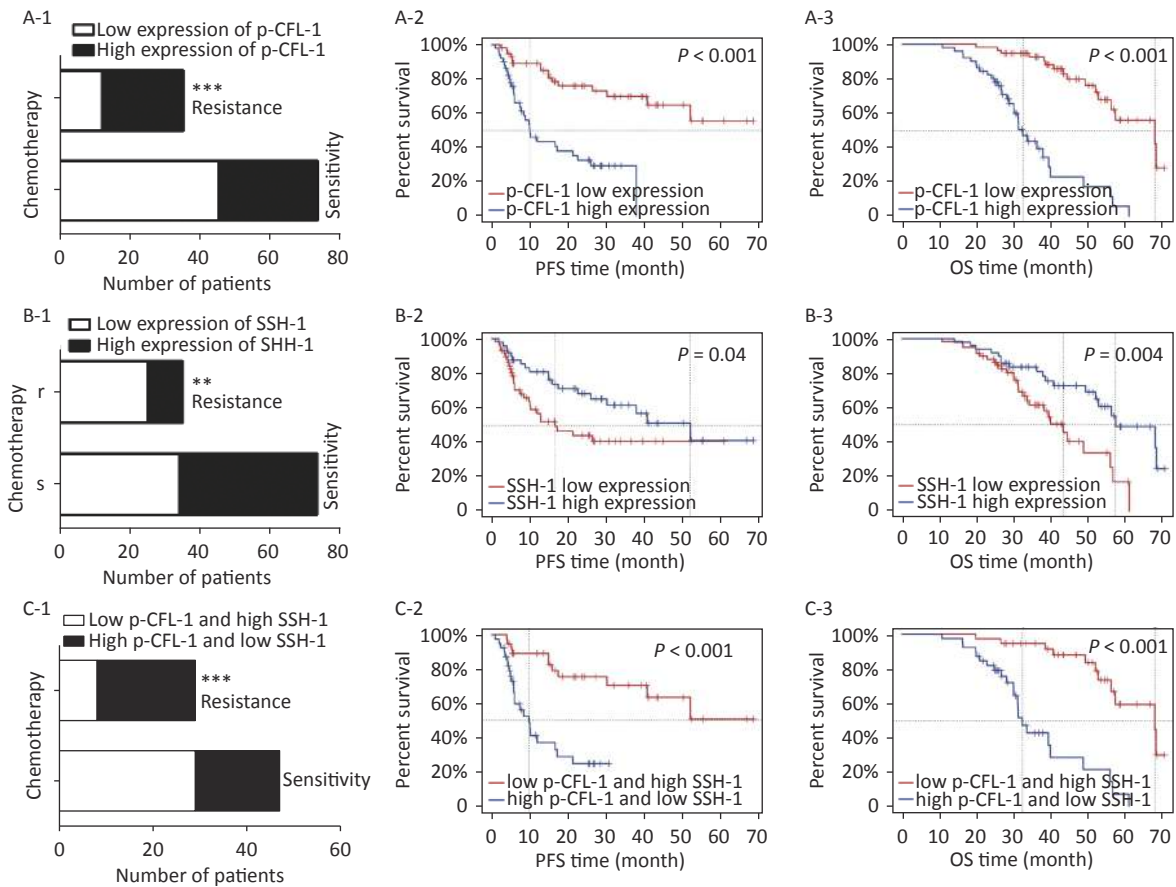


Figure 4. High expression of p-CFL-1 and low expression of SSH-1 in EOC tissues were closely related with the chemotherapy response and prognosis of EOC patients. (A) The effect of different expression levels of p-CFL-1 on the chemotherapy response and prognosis of EOC patients. (A-1) Incidence of high-expression and low-expression of p-CFL-1 in chemo-sensitive ($n = 73$) and chemo-resistant ($n = 35$) patient groups. (A-2, A-3) Kaplan–Meier survival curves of PFS and OS for 108 EOC patients with low and high p-CFL-1 expression. (B) Low expression of SSH-1 was related with chemo-resistance and poor prognosis in EOC patients. (B-1) Incidence of high expression and low expression of SSH-1 in chemo-sensitive ($n = 73$) and chemo-resistant ($n = 35$) patient groups. (B-2, B-3) Kaplan–Meier survival curves of PFS and OS for 108 EOC patients with low and high SSH-1 expression. (C) Coexistence of low expression of SSH-1 and high expression of p-CFL-1 was related to chemo-resistance and poor prognosis in EOC patients. (C-1) Incidence of the coexistence of low expression of SSH-1 and high expression of p-CFL-1 in chemo-sensitive ($n = 73$) and chemo-resistant ($n = 35$) patient groups. (C-2, C-3) Kaplan–Meier survival curves of PFS and OS for 108 EOC patients with both low expression of SSH-1 and high expression of p-CFL-1. EOC patients were dichotomized as low and high expression in relation to the mean value of protein expression. EOC, epithelial ovarian cancer; OS, overall survival; PFS, progression-free survival. * $P < 0.05$; ** $P < 0.01$, *** $P < 0.001$.

significant differences ($\chi^2 = 8.355$, $P = 0.008$) (Figure 4C-1). Spearman's correlation analysis showed that there was a strong negative correlation between the low level of SSH-1 and the high level of p-CFL-1 expression in chemo-resistant patients ($r = -0.725$, $P < 0.001$) and a moderate negative correlation in all patients ($r = -0.415$, $P < 0.001$).

Survival analysis was performed to evaluate the relationship between levels of p-CFL-1 and SSH-1 and clinical outcome. We assessed overall survival (OS) and progression-free survival (PFS). As indicated in Figure 4 and Table 2, a high level of p-CFL-1 was significantly correlated with poor prognosis of patients with median OS shortened by 13 months (chemo-resistant group vs. chemo-sensitive group, 34 vs. 47 months, $P < 0.001$) and PFS shortened by 19 months (8 vs. 26 months, $P < 0.001$), respectively (Figure 4A-2, 4A-3; Table 2). However, high expression of SSH-1 was markedly correlated with better prognosis of patients, with median OS shortened by 14 months (chemo-resistant group vs. chemo-sensitive group, 38 vs. 52 months, $P = 0.004$) and PFS shortened by 20 months (10 vs. 30 months, $P = 0.04$) (Figure 4B-2, 4B-3; Table 2). In addition, patients with both a low level of SSH-1 and a high level of p-CFL-1 showed significantly poorer OS and PFS compared to those with both high SSH-1 and low p-CFL-1 levels (Figure 4C-2, 4C-3; Table 2). These survival data demonstrated that a high level of p-CFL-1 and low level of SSH-1 were closely associated with the poor prognosis of EOC patients.

DISCUSSION

Although a variety of novel therapeutic strategies for EOC have emerged in recent years, the prognosis of EOC has not been markedly improved, especially for patients with chemo-resistance. Explorations of biomarkers predicting chemo-response, the underlying mechanism of chemo-resistance, and measures to reverse such resistance are underway. We previously established an association between

the high level of p-CFL-1 and paclitaxel resistance. In this study, we carried out further experiments to illustrate its mechanistic basis.

Three main findings were obtained in this study. Firstly, a high dose of paclitaxel treatment led to a high cellular level of p-CFL-1 protein, the phosphorylated form of CFL-1 at Ser-3, which induced paclitaxel-resistance. Secondly, cytoplasmic accumulation of p-CFL-1 inhibited mitochondrial apoptosis of EOC cells. Thirdly, SSH-1 silencing was responsible for the overexpression of p-CFL-1 in paclitaxel-resistant EOC cells. Both the low expression of SSH-1 and the high level of p-CFL-1 in EOC tissue, alone or in combination, could predict a likelihood of chemo-resistance and a poor prognosis among EOC patients. Our results suggest an important role for the SSH-1/p-CFL-1 signaling pathway regarding apoptosis inhibition in EOC cell paclitaxel resistance (Figure 5).

Previous studies have documented that CFL-1 is highly correlated with metastasis and invasion of cancer cells^[13,14]. However, our data showed that there was no significant increase in cell migration and invasion with CFL-1 or p-CFL-1 overexpression, although cell migration and invasion was attenuated by knockdown of CFL-1 and downregulation of p-CFL-1 (Supplementary Figure S1 available in www.besjournal.com). It has been suggested that metastasis and invasion is not a key trigger for SKOV3 cell resistance against paclitaxel. Mitochondrial translocation of CFL-1 was reported to induce apoptosis in previous studies, and dephosphorylated CFL-1 is the only form that can be transferred to mitochondria^[17-20]. Our study confirmed that with more phosphorylated CFL-1 in the cytoplasm, less CFL-1 was able to translocate into the mitochondria to induce EOC cell apoptosis, resulting in a build-up of cytoplasmic p-CFL-1 in paclitaxel-resistant cells.

We also established that the p-CFL-1 level positively correlates with the level of Bcl-2, favoring cell survival. Wild-type CFL-1 and the S3D mutant with overexpressed p-CFL-1 enhanced Bcl-2 protein

Table 2. Prognosis of 108 EOC patients with high expression of p-CFL-1 or low expression of SSH-1

Chemotherapy response (n)	p-CFL-1 high expression				SSH-1 low expression			
	OS		PFS		OS		PFS	
	Median time (m)	P value	Median time (m)	P value	Median time (m)	P value	Median time (m)	P value
Chemo-sensitivity (73)	47	< 0.001***	26	< 0.001***	52	0.004**	30	0.04*
Chemo-resistance (35)	34		8		38		10	

Note. * $P \leq 0.05$, ** $P \leq 0.01$ and *** $P \leq 0.001$. OS, overall survival; PFS, progression-free survival.

expression, while the S3A mutant with dephosphorylated CFL-1 decreased Bcl-2 expression. It has been reported that Bcl-2 family proteins are primary regulators of the mitochondrial apoptotic cascade and can be cleaved in cells treated with various concentrations of paclitaxel^[21-23]. Young et al. reported that MCL-1, a pro-survival member of the Bcl-2 family, can directly bind and alter the

phosphorylation of CFL-1 in breast cancer cells^[24,25]. MCL-1 is an important target for cancer therapy and is involved in the drug resistance of many kinds of cancers, including oral cancer^[26], lung cancer^[27,28], pancreatic cancer^[29], ovarian cancer^[28], and breast cancer^[28,30,31]. However, the exact mechanism of apoptosis and chemo-resistance that involves CFL-1 phosphorylation and Bcl-2 will require further

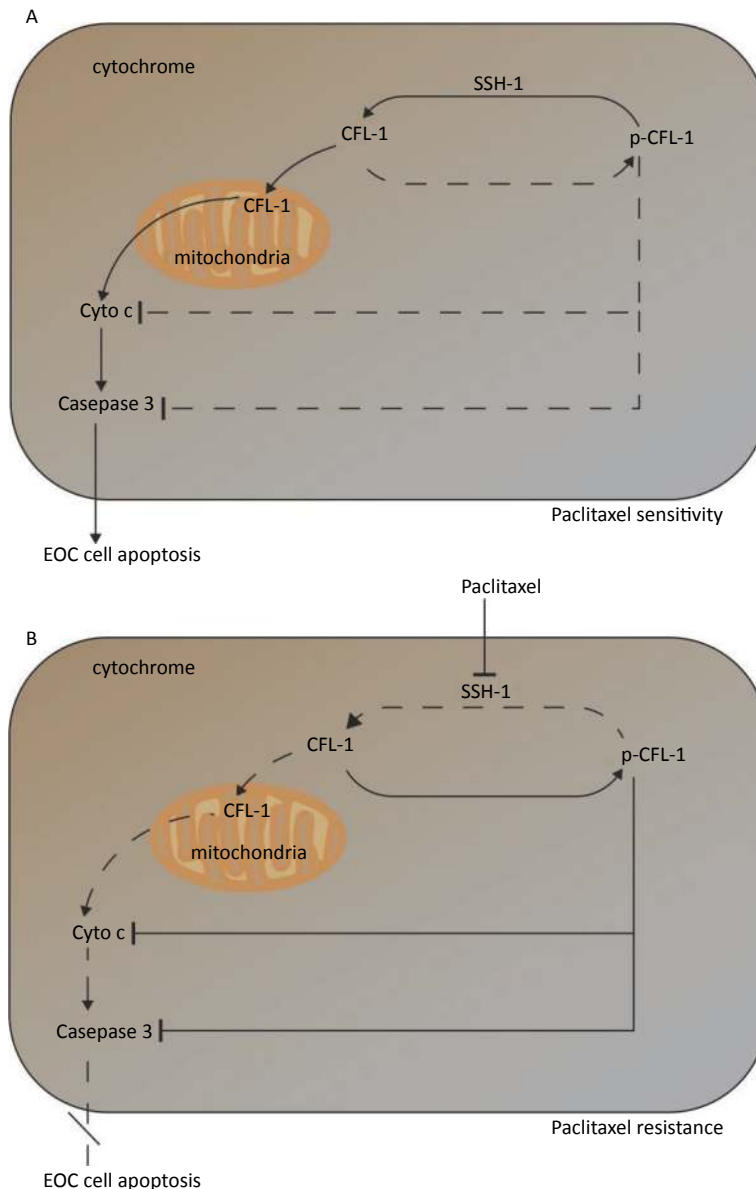


Figure 5. Mechanism of paclitaxel resistance via cytoplasmic p-CFL-1 induced mitochondrial apoptosis. (A) In paclitaxel-sensitive EOC cells, SSH1 modulates CFL-1 dephosphorylation, and dephosphorylated CFL-1 translocates from the cytoplasm to the mitochondria to induce cell apoptosis. (B) In paclitaxel-resistant EOC cells, paclitaxel promotes CFL-1 phosphorylation by suppressing SSH-1 activity. The decrease in mitochondrial dephosphorylated CFL-1 and accumulation of cytoplasmic p-CFL-1 inhibits cell apoptosis, which results in paclitaxel resistance.

investigation.

Finally, we wanted to determine how phosphorylation of CFL-1 was regulated in paclitaxel-resistant EOC cells. Ser-3 is the only site where CFL-1 phosphorylation can be altered by different phosphokinases and phosphatases^[32]. We screened several enzymes that could alter the phosphorylation state of CFL-1 at Ser-3 and observed a significant decrease in the expression of SSH-1 in paclitaxel-resistant EOC cells. The SSH-1 protein, a dual-specificity phosphatase, catalyzes hydrolysis of the Ser-3 phosphate group in phosphorylated CFL-1^[33-36]. SSH-1 has been implicated in cell migration, protrusion, and mitosis, contributing to the metastasis, migration, and poor prognosis of breast and colorectal cancers^[37-39]. To the best of our knowledge, the effect of the SSH-1/p-CFL-1 pathway on chemotherapy resistance of EOC has not been reported. Our results revealed a negative correlation between the expression of SSH-1 and p-CFL-1 in the mechanism of paclitaxel resistance for the first time. In addition, our data revealed that SSH-1/p-CFL-1 signaling was strongly correlated with survival and the chemo-response in EOC patients, consistent with the *in vitro* results, indicating that SSH1/pCFL1 signaling can serve as a predictor for chemo-resistance and EOC progression.

There are three limitations of this study. First, we adopted a retrospective single-center design. Second, it remains to be determined whether there is feedback regulation of SSH-1 and p-CFL-1, i.e., whether SSH-1 unidirectionally dephosphorylates p-CFL-1 or p-CFL-1 also regulates the expression of SSH-1. Finally, the specific mechanism of SSH-1/p-CFL-1-induced apoptosis requires further investigation. Therefore, whether p-CFL-1 is an independent prognostic biomarker of paclitaxel resistance, and whether the SSH-1/p-CFL-1 signaling pathway can be a target to reverse paclitaxel resistance will require further investigation.

CONCLUSIONS

We elucidated a novel mechanism underlying chemo-resistance mediated by CFL-1 phosphorylation. Downregulation of SSH-1 can promote the stability of p-CFL-1 in the cytoplasm, inhibit apoptosis, and further promote paclitaxel-resistance, which leads to poor prognosis in EOC patients.

LIST OF ABBREVIATIONS

EOC, epithelial ovarian cancer; CFL-1, cofilin-1;

SSH-1, Slingshot-1; Bcl-2, B-cell lymphoma-2; OS, overall survival; PFS, progression-free survival; IC50, half-maximal inhibitory concentration; WB, western blot; CCK-8, Cell Counting Kit-8; qRT-PCR, quantitative real-time polymerase chain reaction; IHC, immunohistochemistry.

AUTHORS' CONTRIBUTIONS

Conceptualization and methodology: LM; formal analysis and data curation: LM, ZW, CD, HS, and LHY; validation and investigation: LM, DXD, and LQB; original draft preparation and revisions: LM and YCX. All authors read and approved the final manuscript.

CONFLICT OF INTERESTS

The authors declare that they have no competing interests.

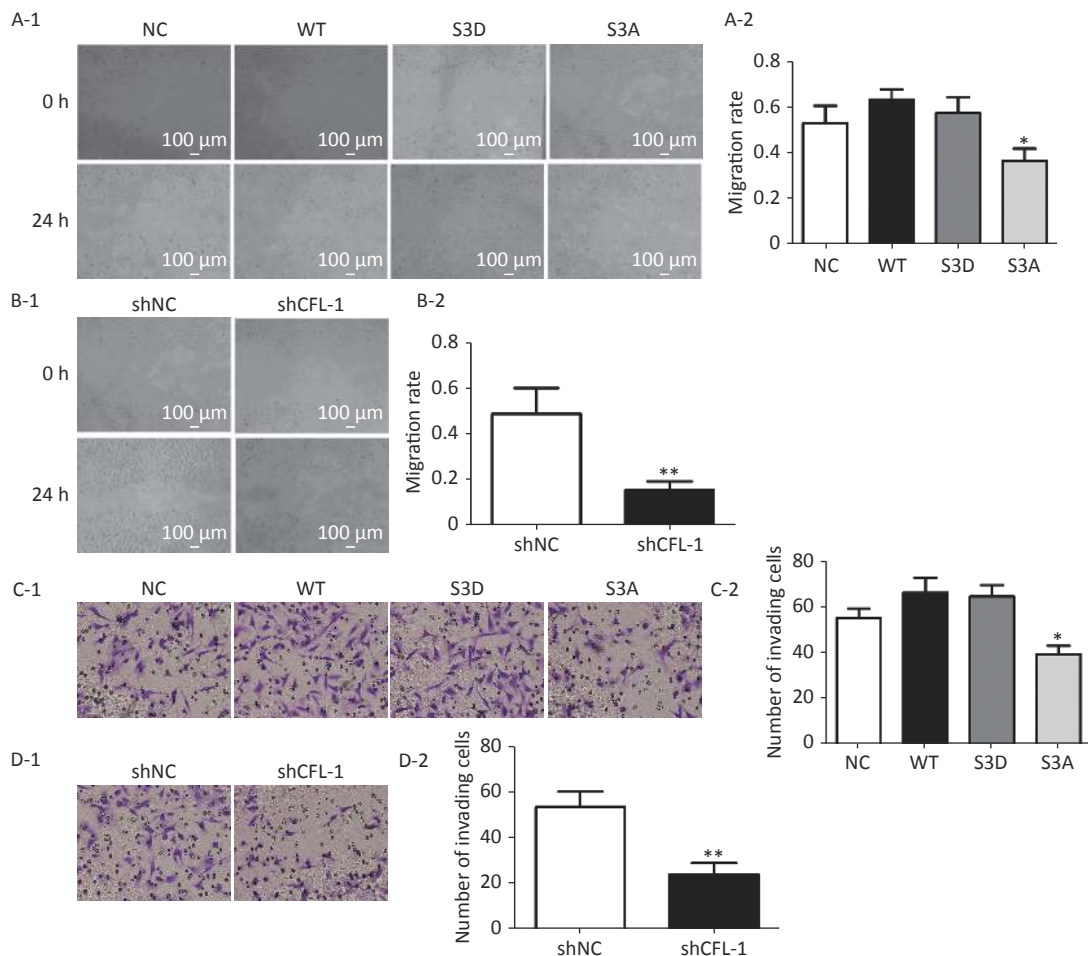
Received: March 1, 2021;

Accepted: May 17, 2021

REFERENCES

- Torre LA, Trabert B, DeSantis CE, et al. Ovarian cancer statistics, 2018. *CA Cancer J Clin*, 2018; 68, 284–96.
- Eisenhauer EA. Real-world evidence in the treatment of ovarian cancer. *Ann Oncol*, 2017; 28, viii61–5.
- Narod S. Can advanced-stage ovarian cancer be cured? *Nat Rev Clin Oncol*, 2016; 13, 255–61.
- Buechel M, Herzog TJ, Westin SN, et al. Treatment of patients with recurrent epithelial ovarian cancer for whom platinum is still an option. *Ann Oncol*, 2019; 30, 721–32.
- Stuart GCE. First-line treatment regimens and the role of consolidation therapy in advanced ovarian cancer. *Gynecol Oncol*, 2003; 90, S8–15.
- Moufarrij S, Dandapani M, Arthofer E, et al. Epigenetic therapy for ovarian cancer: promise and progress. *Clin Epigenetics*, 2019; 11, 7.
- Li M, Yin J, Mao N, et al. Upregulation of phosphorylated cofilin 1 correlates with taxol resistance in human ovarian cancer *in vitro* and *in vivo*. *Oncol Rep*, 2013; 29, 58–66.
- Mizuno K. Signaling mechanisms and functional roles of cofilin phosphorylation and dephosphorylation. *Cell Signal*, 2013; 25, 457–69.
- Shishkin S, Eremina L, Pashintseva N, et al. Cofilin-1 and Other ADF/Cofilin Superfamily Members in Human Malignant Cells. *Int J Mol Sci*, 2016; 18.
- Aggelou H, Chadla P, Nikou S, et al. LIMK/cofilin pathway and Slingshot are implicated in human colorectal cancer progression and chemoresistance. *Virchows Arch*, 2018; 472, 727–37.
- Hoffmann L, Rust MB, Culmsee C. Actin(g) on mitochondria - a role for cofilin1 in neuronal cell death pathways. *Biol Chem*, 2019; 400, 1089–97.
- Kolegova ES, Kakurina GV, Kondakova IV, et al. Adenylate Cyclase-Associated Protein 1 and Cofilin in Progression of Non-Small Cell Lung Cancer. *Bull Exp Biol Med*, 2019; 167, 393–95.
- Lee M-H, Kundu JK, Chae J-I, et al. Targeting

- ROCK/LIMK/cofilin signaling pathway in cancer. *Arch Pharm Res*, 2019; 42, 481–91.
14. Wang F, Wu D, Xu Z, et al. miR-182-5p affects human bladder cancer cell proliferation, migration and invasion through regulating Cofilin 1. *Cancer Cell Int*, 2019; 19, 42.
 15. Qin Y, Li W, Long Y, et al. Relationship between p-cofilin and cisplatin resistance in patients with ovarian cancer and the role of p-cofilin in prognosis. *Cancer Biomark*, 2019; 24, 469–75.
 16. Li M, Shi J, Zou L, et al. The relationship between phosphorylation at Ser3 of cofilin and Taxol resistance of ovarian cancer in elderly female patients. *Chinese Journal of Geriatrics*, 2017; 2.
 17. Liao PH, Hsu HH, Chen TS, et al. Phosphorylation of cofilin-1 by ERK confers HDAC inhibitor resistance in hepatocellular carcinoma cells via decreased ROS-mediated mitochondria injury. *Oncogene*, 2017; 36, 1978–90.
 18. Tang Q-F, Sun J, Yu H, et al. The Zuo Jin Wan Formula Induces Mitochondrial Apoptosis of Cisplatin-Resistant Gastric Cancer Cells via Cofilin-1. *Evid Based Complement Alternat Med*, 2016; 2016, 8203789.
 19. Wabnitz GH, Goursot C, Jahraus B, et al. Mitochondrial translocation of oxidized cofilin induces caspase-independent necrotic-like programmed cell death of T cells. *Cell Death Dis*, 2010; 1, e58.
 20. Chua BT, Volbracht C, Tan KO, et al. Mitochondrial translocation of cofilin is an early step in apoptosis induction. *Nat Cell Biol*, 2003; 5, 1083–9.
 21. Matuszyk J, Klopotoska D. miR-125b lowers sensitivity to apoptosis following mitotic arrest: Implications for breast cancer therapy. *J Cell Physiol*, 2020; 235, 6335–44.
 22. Nair PR. Delivering Combination Chemotherapies and Targeting Oncogenic Pathways via Polymeric Drug Delivery Systems. *Polymers (Basel)*, 2019; 11.
 23. Park S-J, Wu C-H, Gordon JD, et al. Taxol induces caspase-10-dependent apoptosis. *J Biol Chem*, 2004; 279, 51057–67.
 24. Young AI, Timpson P, Gallego-Ortega D, et al. Myeloid cell leukemia 1 (MCL-1), an unexpected modulator of protein kinase signaling during invasion. *Cell Adh Migr*, 2018; 12, 513–23.
 25. Young AJ, Law AMK, Castillo L, et al. MCL-1 inhibition provides a new way to suppress breast cancer metastasis and increase sensitivity to dasatinib. *Breast Cancer Res*, 2016; 18, 125.
 26. Palve V, Mallick S, Ghaisas G, et al. Overexpression of Mcl-1L splice variant is associated with poor prognosis and chemoresistance in oral cancers. *PLoS One*, 2014; 9, e111927.
 27. Toge M, Yokoyama S, Kato S, et al. Critical contribution of MCL-1 in EMT-associated chemo-resistance in A549 non-small cell lung cancer. *Int J Oncol*, 2015; 46, 1844–48.
 28. Wertz IE, Kusam S, Lam C, et al. Sensitivity to antitubulin chemotherapeutics is regulated by MCL1 and FBW7. *Nature*, 2011; 471, 110–14.
 29. Wei D, Zhang Q, Schreiber JS, et al. Targeting mcl-1 for radiosensitization of pancreatic cancers. *Transl Oncol*, 2015; 8, 47–54.
 30. Balko JM, Giltne JM, Wang K, et al. Molecular profiling of the residual disease of triple-negative breast cancers after neoadjuvant chemotherapy identifies actionable therapeutic targets. *Cancer Discov*, 2014; 4, 232–45.
 31. Xiao Y, Nimmer P, Sheppard GS, et al. MCL-1 Is a Key Determinant of Breast Cancer Cell Survival: Validation of MCL-1 Dependency Utilizing a Highly Selective Small Molecule Inhibitor. *Mol Cancer Ther*, 2015; 14, 1837–47.
 32. Moriyama K, Iida K, Yahara I. Phosphorylation of Ser-3 of cofilin regulates its essential function on actin. *Genes Cells*, 1996; 1, 73–86.
 33. Nishita M, Wang Y, Tomizawa C, et al. Phosphoinositide 3-kinase-mediated activation of cofilin phosphatase Slingshot and its role for insulin-induced membrane protrusion. *J Biol Chem*, 2004; 279, 7193–98.
 34. Huang TY, DerMardirossian C, Bokoch GM. Cofilin phosphatases and regulation of actin dynamics. *Curr Opin Cell Biol*, 2006; 18, 26–31.
 35. Niwa R, Nagata-Ohashi K, Takeichi M, et al. Control of actin reorganization by Slingshot, a family of phosphatases that dephosphorylate ADF/cofilin. *Cell*, 2002; 108, 233–46.
 36. Eiseler T, Döppler H, Yan IK, et al. Protein kinase D1 regulates cofilin-mediated F-actin reorganization and cell motility through slingshot. *Nat Cell Biol*, 2009; 11, 545–56.
 37. Peterburs P, Heering J, Link G, et al. Protein kinase D regulates cell migration by direct phosphorylation of the cofilin phosphatase slingshot 1 like. *Cancer Res*, 2009; 69, 5634–38.
 38. Chen C, Maimaiti Y, Zhijun S, et al. Slingshot-1L, a cofilin phosphatase, induces primary breast cancer metastasis. *Oncotarget*, 2017; 8, 66195–203.
 39. Song X, Xie D, Xia X, et al. Role of SSH1 in colorectal cancer prognosis and tumor progression. *J Gastroenterol Hepatol*, 2020; 35, 1180–8.



Supplementary Figure S1. Effect of p-CFL-1 on the migration and invasion of ovarian cancer cells. Description of data: (A-1), (A-2) A scratch wound-healing assay was performed to evaluate the effect of p-CFL-1 on cell migration. Representative images of migration of SKOV3 cells transfected with WT, S3D, S3A, or vector in a scratch wound-healing assay are shown in the left panel. (B-1), (B-2) A scratch wound-healing assay was performed to evaluate the migration of SKOV3 cells with CFL-1 knockdown. Scale bar: 100 μ m. The bar graphs show mean \pm SD of migration rate of wounds from three independent experiments (right panel) (* P < 0.05, ** P < 0.05). (C-1), (C-2) A Transwell assay was performed to evaluate the invasion of cells with different levels of p-CFL-1. (D-1), (D-2) A scratch wound-healing assay was performed to evaluate the migration of SKOV3 cells with knockdown of CFL-1. Representative images of cell invasion are shown (left panel). The bar graphs show mean \pm SD of the numbers of invading A2780 and SKOV3 cells from three independent experiments (right panel) (* P < 0.05, ** P < 0.05). Scale bar: 100 μ m. Images shown are representative of three independent experiments.